Green electroluminescence from radial m -plane InGaN quantum wells grown on GaN wire sidewalls by metal–organic vapor phase epitaxy

Akanksha Kapoor, Nan Guan, Martin Vallo, Agnès Messanvi, Lorenzo Mancini, Eric Gautier, Catherine Bougerol, Bruno Gayral, François H. Julien, François Vurpillot, et al.

Green electroluminescence from radial *m*-plane InGaN quantum wells grown on GaN wire sidewalls by MOVPE

Akanksha KAPOOR [1, a)], Nan GUAN[2], Martin VALLO[1], Agnes MESSANVI[1, 2], Lorenzo MANCINI[2,3], Eric GAUTIER[4], Catherine BOUGEROL[5], Bruno GAYRAL[1], Francois H. JULIEN[2], Lorenzo RIGUTTI[3], Maria TCHERNYCHEVA[2], Joël EYMERY[6] and Christophe DURAND[1]

[1] *Univ. Grenoble Alpes, CEA, INAC-Pheliqs, 38000 Grenoble, France*

[2] *Center for Nanoscience and Nanotechnology (C2N), UMR 9001 CNRS, Bat. 220, University Paris-Sud, Univ. Paris-Saclay, 91405 Orsay, Cedex*

[3] *Normandie Univ., GPM, UNIROUEN, INSA Rouen, CNRS, 76000 Rouen, France.*

[4] *Univ. Grenoble Alpes, CEA, INAC-Spintec, 38000 Grenoble, France*

[5] *Univ. Grenoble Alpes, CNRS, Institut Néel, 38000 Grenoble, France*

[6] *Univ. Grenoble Alpes, CEA, INAC-MEM, 38000 Grenoble, France*

a) Author to whom correspondence should be addressed*: akanksha.kapoor@cea.fr*

Keywords: Nanowires, green emission, LED, MOVPE, nitride semiconductors

Abstract

We demonstrate green emission from InGaN/GaN multiple quantum wells (MQWs) grown on *m*-plane sidewalls of GaN wires. To tune the emission wavelength, InGaN radial wells were grown by metal-organic vapor phase epitaxy (MOVPE) at decreasing temperatures ranging from 710 down to 620°C to increase the In incorporation. A comprehensive investigation combining structural and optical analyses demonstrates that the green emission from the non-polar *m*-plane wire sidewalls is achieved for the wells grown at 650°C (namely, for 2.7 nm-thick wells sandwiched by 11 nm-thick GaN barriers). The observed emission wavelength of 500-550 nm is consistent with an average In-content of MQWs measured in the range of 24 ± 4 % by atom probe tomography. Single wires were electrically contacted and the green electroluminescence from *m*-plane facets was established on single wire-LED devices. This demonstrates the possibility to produce green emitters with core-shell wire LEDs elaborated by industrial and scalable MOVPE technique.

The GaN nanowire geometry offers a new 1D-template to develop nitride devices compared to standard planar growths of nitride semiconductors. GaN nano/microwires covered with InGaN/GaN multiple quantum wells (MQWs) have attracted a lot of interest mainly focused on the fabrication of efficient light emitting diodes (LEDs).[1] Regardless of the high efficiency issue in the nanowire-based LEDs, the 1D-geometry offers key advantages for device applications: growth on various low-cost substrates (Si, silica, metal foils, graphene)[2–6], high quality crystal structure with strain relaxation and/or dislocation bending in the wire foot part,[7,8] much larger active surface area in the case of core/shell MQWs[1,9] and achievement of fully flexible and transparent devices by peeling off the nanowires encapsulated in polymer films.[10–12]

Although the long wavelength emission up to red color has already been achieved by axial InGaN/GaN MQWs grown by molecular beam epitaxy (MBE),[13–16] such colors are highly challenging to achieve by the usual industrial method, i.e. Metal-Organic Vapor Phase Epitaxy (MOVPE). The fabrication of wire-based LEDs using core-shell InGaN/GaN MQWs grown by MOVPE is now well established for the blue emission.[17–19] However, the green emission that requires In-rich InGaN/GaN MQWs seems far to be straightforward for the core-shell geometry due to the usually lower In incorporation on *m*-plane surfaces corresponding to the wire sidewalls with respect to the usual *c*-plane orientation. Indeed, we observed that the In-content in two different MQW systems grown using the strictly same growth conditions results in 2-4 % less incorporation on *m*-plane than on *c*-plane surfaces: 15% *vs* 18,5% for InGaN[20] and 15% *vs* 17-18% for InAlN.[21] According to the literature, electroluminescence in long wavelength colors (from green to red) are reported for pencil-shaped Ga-polar GaN wires grown by MOVPE and covered by InGaN/GaN MQWs. Higher In-incorporation in MQWs is observed on the *c*-plane flat surface corresponding to truncated pyramidal shape located on the nanowire apex (the *c*-plane flat area can be tuned with growth

conditions[22] and longer wavelength emission is favored when the area of *c*-facet is reduced[23]). Also, a higher In-content is observed on the boundaries between the hexagonal and the pyramidal edges.[23] These localized zones with a higher In-content leads to a green/red electroluminescence emission at low current injection in nanowire-LED devices, but the light tune to the blue color at higher current injection.[24,25] Consequently, the long wavelength emission is located on the upper part of the Ga-polar GaN wires, whereas the *m*-plane InGaN/GaN MQWs located along wire sidewalls emit a standard blue color that is activated at high current injection.[25]

This work reports the demonstration of the green luminescence from *m*-plane MQWs formed on the wire sidewalls by MOVPE growth technique. The growth of InGaN/GaN MQWs in a core-shell structure at different temperatures (710 – 620 °C) is analyzed. The decrease of the growth temperature boosts the In incorporation as evidenced by optical and structural analyzes. The MQWs with In-content higher than 20% on the *m*-plane sidewalls of the N-polar GaN wires are achieved and used to demonstrate MOVPE-grown single wire LEDs emitting green light in the 500 – 550 nm range.

Self-assembled N-polar *c*-GaN wires with core-shell InGaN/GaN MQWs were grown by MOVPE on nitridated *c*-sapphire substrates in a close-couple showerhead reactor, as depicted in Figure 1(a). Contrary to Ga-polar GaN wires having a pyramidal apex, the N-polar wire ones present a flat *c*-plane facet on the wire top.[26] The growth method involves low V/III ratio (~50), high flux of silane (~200 nmol/min), high temperature (1050 °C) and high pressure (800 mbar).[27] The high flux of silane promotes the vertical growth of n^+-doped GaN (300 s of growth gives ~10 μm length) thanks to the formation of an ultra-thin passivation layer of SiN_x around the stem of the GaN core.[28,29] The silane addition is then stopped so as to grow an unintentionally doped GaN (u-GaN) wire (~15 μm for 300 s growth time) as can be seen in the schematics of Figure 1(a). This step is followed by the radial growth of seven InGaN

quantum wells (QWs) separated by GaN barriers around the GaN wires at 400 mbar. Four different samples were grown by varying only the growth temperature of the QWs (710, 685, 650 and 620 °C) keeping constant the barrier temperature at 885°C. The temperature evolution with the growth time for InGaN/GaN QWs is illustrated in Figure 1(b), where the decrease in the growth temperature of InGaN QWs is followed by a rapid increase in the constant growth temperature of the GaN barriers. The last growth step corresponds to the 70 nm-thick p-doped GaN shell at 920°C followed by a dopant activation annealing at 700°C during 20 min.

Figure 2 shows scanning electron microscopy (SEM) images (bird and cross-section views) of as-grown samples performed at various QW growth temperatures. The wire average density is 10^6 wire/cm^2, while the diameter and length of the GaN core are in the range of (0.65–1.2 µm) and (28 – 33 µm), respectively. Interestingly, the core-shell geometry of InGaN/GaN MQWs is preserved for all samples, even for the sample synthesized at the lowest temperature. The main difference is the degradation of the SiN_x selectivity on the bottom n^+-GaN part of the wires. Residual over-growths are especially visible for the sample grown at 620°C that can be attributed to a lower diffusion length of adatoms.

Microstructural analyses of the 650°C–QW sample has been carried out by Scanning Transmission Electron Microscopy (STEM) using a High Angle Annular Dark Field detector (HAADF) to emphasize the chemical contrast (Z-contrast) on the images. The experiments have been performed on a FEI OSIRIS microscope operated at 200 kV and equipped with four silicon drift detectors to record also Energy Dispersive X-ray (EDX) chemical maps. Thin slices of the wires have been cut perpendicular to the growth *c*-axis by ultra-microtomy using a diamond blade.[30] Figure 3(a) shows a part of one wire slice where the 7 QWs appear in bright, whereas the GaN parts (barriers and p-GaN shell) are in dark. In the high resolution enlarged TEM image (Fig. 3(b)), the measured thicknesses of the QWs and barriers are 2.7

nm and 11 nm, respectively (except for the first QW, which is somewhat larger), while that of the p-doped GaN shell is about 70 nm. Note that some faint white lines visible in Fig. 3(a,b), originating from the interface between the GaN core and the first InGaN QW, propagate through the whole InGaN/GaN structure. Similar features have been already reported in MQWs core-shell structures and have been identified as stacking faults.[17,31] Figure 3(c) shows the spatial distribution of Ga, In and N from EDX analyses measured inside the red rectangle shown in Fig. 3(a), while Figure 3(d) depicts the In profile measured in the dash-line rectangle shown in the EDX mapping (Fig. 3(c)) as a function of the position from the innermost QW to the last QW. Note that the uncertain values for the thicknesses of the QW obtained from the profile is due to the lack of enough spatial resolution in these maps. Thus, the average percentage of In content inside the seven QWs obtained by EDX profile is in the order of 20 % and stay almost constant in the range of ±2% whatever the QW. We consider that this value is underestimated due to the teardrop-shaped volume of the e-beam excitation along the slice width leading to overestimation of Ga content coming from the barriers. These maps have not enough spatial resolution to detect any In-composition fluctuation that might exist at the atomic scale. These observations were therefore combined with atom probe tomography (APT) experiments performed on the same sample. APT was performed in a CAMECA laser assisted wide angle tomographic atom probe (LAWATAP) under conditions similar to those adopted for the analysis of InGaN/GaN *m*-plane QWs in the previous works (the tip preparation perpendicular to the *m*-plane sidewall surfaces is performed by focused ion beam technique).[32,31] Fig. 3(e) shows the 2D cross-sectional view of the reconstructed positions of the In atoms within all the seven QWs. The similar cross-sectional and top view for a 2 nm thick slice of the innermost QW are shown in Fig. 3(f), while the In mapping to quantify the In content within the QW volume is depicted in Fig. 3(g). As can be seen, the In-content is non-uniformly distributed exhibiting a sequence of In-rich and In-poor bands

aligned along the *a*-axis direction possibly related to the local perturbation induced by stacking faults.[17] Further, the mapping also reveals red zones with high In-content up to 30% related to strongly inhomogeneous In-composition in the QW for an average In composition estimated about 23%. However, the In profile for a 25 nm x 25 nm cross section along the seven QWs shown in Fig. 3(h) exhibits an In-composition around 25% with a variation of 2.5 % from well-to-well. From this APT analysis, we can estimate an average In-content between 22(±2)% and 27(±2)% in the QWs, leading to a average value around 24(±4)%. Basically, the In profile measured both by EDX and APT techniques evidences a In content higher than 20% required for green emission originating from *m*-plane InGaN/GaN core-shell MQWs using a growth temperature as low as 650°C to enhance the In incorporation

The crystal orientation is known to have a significant impact on the MQW growth (growth rate and In composition)[33], nevertheless no clear tendency about the In incorporation is reported in the literature on *m*-plane surfaces regarding the *c*-plane orientation[34] due to the strong dependence on growth conditions.[35] In the case of MOVPE, Horenburg *et al.* recently reported that In incorporation is strongly dependent on the strain state of the *m*-plane InGaN/GaN MQW systems by adding an InAlN buffer layer either lattice-matched along the *c*-axis or *a*-axis.[36] The higher In incorporation corresponds to the situation having the *c*-axis lattice matched and an elastic strain along the *a*-axis. Also, the high growth rate of InGaN limits the In desorption resulting in a higher In-content inside the QWs.[37] Consequently, the In incorporation higher than 20% on *m*-plane sidewalls certainly results from a high growth rate of the InGaN QWs (estimated at 0.7 Å/s) combined with a favorable strain state.

The optical characterization of all the samples was performed at low temperature (5 K) using photoluminescence (PL) and cathodoluminescence (CL) spectroscopy on ensembles of wires dispersed on silicon substrates. The PL experiment was performed by exciting wires at 244 nm using a continuous laser diode with fixed excitation power about 0.5 mW. Figure 4(a)

shows the behavior of normalized PL spectra as a function of QW growth temperature. A red shift can be observed from 407 to 550 nm for QWs grown at temperatures from 710 to 620 °C, which can be attributed to an increase of the In incorporation associated with a lower growth temperature. The sample with QWs grown at 650 °C exhibits a significantly large emission peak centered at 510 nm corresponding to a green emission. Such emission is consistent with the estimated In-content (24 ±4%) in the radial QWs for this sample. It can also be noted that the maximum of intensity decreases accompanied with a peak broadening as the growth temperature decreases to 620°C. Assuming a similar density of dispersed wires, the intensity decrease may correspond to the presence of structural defects in the QWs.[38] The large peak broadening (~ 300 meV) is attributed to the strong inhomogeneity of In observed by APT mappings. The peak observed at 3.4 eV (352 nm) is attributed to the near band edge of highly n^+-doped core GaN segment present in all the samples.[27] Figure 4(b) shows temperature-dependence PL spectra for the sample with QWs grown at 650 °C. The green emission dominates at low temperature, while two other contributions close to 400 and 550 nm are attributed to the blue residual emission and the yellow band defect emission, respectively. The inset of Fig. 4(b) shows the Arrhenius plot of the integrated intensity as a function of 1000/T, which allows estimating an activation energy $E_a \approx 22$ meV. This value is consistent with the reported values for green emission *c*-plane MQWs,[39] which is related to localization effects.[40] In addition to PL measurements, CL mapping was performed in order to understand the spatial localization of the different spectral contributions of the luminescence. Figure 4(c) depicts spectrally filtered CL maps of typical wires with QWs grown at 710, 685 and 650 °C (dark area corresponds to light emission). Firstly, it can be clearly seen that the near band edge emission of GaN (350 nm-CL maps) arises from the n^+-GaN wire base part, while the emission for wavelengths above 400 nm mainly comes from the active regions of the wire corresponding to the QWs. The samples with QW grown at 710 and 685 °C emit

blue light as detected in the 450 nm-CL maps, contrary to the sample with QW made at 650°C that emits only green light (visible in the 500 nm-CL maps). This emission at 500 nm is consistent with the above-described PL results, showing that the indium content is high enough to cause the green emission. The yellow band emission related to deep-defects centered at ~550 nm is visible in all samples and is attributed to the upper u-GaN part of wires, as previously reported.[27] For the QWs grown at 650 °C, the CL mapping at 500 nm highlights unambiguously that the green emission comes from the *m*-plane wire sidewalls.

Single wire LEDs were fabricated from 650°C-QW sample for optoelectronic characterizations following a procedure previously described in Ref. [41]. The wires were mechanically detached from their native substrate and dispersed on a SiO_2(300nm)/Si templates. Because of a relatively large wire diameter, hydrogen silsesquioxane (HSQ) was spin-coated and then annealed to provide a SiO_x buffer layer supporting metal contacts. The wire surface was cleaned from the HSQ residues by wet-etching with diluted HF. Two steps of e-beam lithography were performed to define the metal contacts on the shell and on the core (Ni/Au for the shell p-contact and Ti/Al/Ti/Au for the core n-contact) followed by a lift-off procedure. Fig. 5(a) shows an SEM image of a single nanowire device. Finally, micro-bonding was used to contact the wire-LEDs. The current-voltage (I-V) characteristics of single nanowire devices were measured by a Keithley 2636 source meter. Typical room temperature I-V curve is shown in Fig. 5(b). It has a rectifying behavior characteristic of an LED with a turn-on voltage of about 5 V. This relatively high turn-on voltage is due to the Schottky nature of the p-contact (no annealing of the Ni/Au contact was performed, since a degradation of the Ni/Au adhesion to the HSQ buffer after annealing was observed in previous unsuccessful fabrication runs). The devices show a low leakage under reverse bias (at -20 V the reverse current is only 10 nA). This low reverse leakage demonstrates that the active region with QWs grown at 650 °C exhibits a good material quality. Room temperature

electroluminescence (EL) spectra under different injection currents are shown in Fig. 5(c). A measureable EL signal starts to appear around 100 – 150 nA. The spectra are peaked at 534 nm (2.32 eV) with an important broadening of 221 meV. The observed emission wavelength is consistent with the PL results, however the peak broadening is lower than the one observed in PL (220 meV for EL *vs.* 300 meV for PL). This difference is attributed to the additional contribution of the yellow band emission tail to the broadening of the PL spectra, whereas the yellow band should not be excited in EL experiments. Only a small blue shift of the peak wavelength from 544 to 534 nm can be observed for small currents (from 150 to 200 nA) and then for currents above 200 nA the peak wavelength and the spectral shape remain unchanged. We remind that for previous realizations of red/green luminescence reported in the literature using pencil-like nanowires, a strong blueshift of EL was systematically observed.[25] It was ascribed to the variation of current injection path, which first goes in the In-rich wire apex and then spreads over the *m*-plane sidewalls. This strong blueshift is absent in the present device. The observed stability of the EL wavelength with current is consistent with the attribution of this emission to the *m*-plane MQWs with unchanged distribution of current lines with applied bias.[42] The evolution of the external quantum efficiency (EQE) defined as the spectrally-integrated EL intensity divided by the injected electrical current with injected current is plotted in Fig. 5(d). The EQE first increases following the saturation of non-radiative Shockley-Read-Hall recombination, reaches a maximum at 500 nA (corresponding to a current density of 0.56 A/cm^2, if the total surface of the 6 facets of the p-GaN shell is assumed to contribute to the current) and then remains relatively stable in the analyzed current range.

In summary, the detailed experimental analysis correlating structural, optical as well as electrical measurements presents the possibility of achieving green emission of *m*-plane InGaN/GaN MQWs grown on GaN wire sidewalls in core-shell geometry by MOVPE. The

In-content estimated to be 24% in the wire sidewalls leads to a green electroluminescence highlighting the potential of core-shell wire-based LEDs produced by industrial MOVPE technique to emit long wavelength light.

Acknowledgments:

The authors thank Nicolas Mollard and Pierre-Henri Jouneau from PFNC Minatec for their support in microtomy and EDX measurements respectively. This work has been financially supported by ANR-14-CE26-0020-01 project “PLATOFIL”, ANR-13-JS10-0001-01 project “TAPOTER”, EU H2020 ERC project “NanoHarvest” (grant no. 639052), and French national Labex GaNex (ANR-11-LABX-2014).

Figure Caption:

FIG. 1: (a) Schematics of the core-shell MQWs grown on GaN wire sidewalls, (b) Growth temperature evolution as a function of growth time showing the decreasing temperature for InGaN quantum wells keeping constant the growth temperature of the GaN barriers.

FIG. 2: SEM images of as-grown nanowires with QWs grown at different temperatures: (a) 620°C, (b) 650°C, (c) 685°C and (d) 710°C.

FIG. 3: Structural characterization of the 650°C-QW sample. (a) Transversal cross-sectional STEM-HAADF images taken along the *c*-zone axis depicting the seven quantum wells separating the core and p-GaN, (b) High resolution enlarged STEM-HAADF image showing distinctively the InGaN QWs and GaN barriers, (c) STEM-EDX elemental map for spatial distribution of Ga, In and N in the core-shell heterostructures, (d) Indium profile as a function of position from the 1^{st} QW to 7^{th} QW measured by EDX, (e) APT reconstructed positions of In atoms in seven radial MQWs, (f) Focus on APT reconstructed In atoms along cross-sectional and top view of the innermost QW, (g) 2D map of In composition measured by APT extracted from the 1^{st} QW, (h) In composition profile from the 1^{st} QW to 7^{th} QW measured by APT.

FIG. 4: Optical characterization. (a) Normalized PL spectra at 5K for all the samples with wires dispersed on silicon, (b) PL spectra of the sample with QWs grown at 650°C as a function of temperature. The inset shows the experimental values and the fit of the integrated intensity *vs.* 1000/T, (c) SEM images and CL mappings at 350, 400, 450, 500 and 550 nm for typical single wires corresponding to QWs grown at 710, 685 and 650 °C.

FIG. 5: Wire-LED device based on the 650°C-QW samples. (a) SEM image of a typical single wire-LED device with metal contacts, (b) Room temperature I-V curve of the single nanowire LED in linear scale, inset shows the I-V curve in logarithmic scale, (c) Room temperature EL spectra of the single nanowire LED under different injection currents from 150 nA to 800 nA (Inset: optical image of the operating single nanowire LED), (d) Room-temperature EQE of the single wire-LED as a function of injection current.

Bibliography:

[1] S. Li and A. Waag, J. Appl. Phys. **111**, 71101 (2012).

[2] D. Salomon, A. Dussaigne, M. Lafossas, C. Durand, C. Bougerol, P. Ferret, and J. Eymery, Nanoscale Res. Lett. **8**, 61 (2013).

[3] S. Kang, A. Mandal, J.H. Chu, J. Park, S. Kwon, and C.-R. Lee, Sci. Rep. **5**, 10808 (2015).

[4] V. Kumaresan, L. Largeau, F. Oehler, H. Zhang, O. Mauguin, F. Glas, N. Gogneau, M. Tchernycheva, and J.-C. Harmand, Nanotechnology **27**, 135602 (2016).

[5] V. Kumaresan, L. Largeau, A. Madouri, F. Glas, H. Zhang, F. Oehler, A. Cavanna, A. Babichev, L. Travers, N. Gogneau, M. Tchernycheva, and J.C. Harmand, Nano Lett. **16**, 4895 (2016).

[6] B.J. May, A.T.M.G. Sarwar, and R.C. Myers, Appl. Phys. Lett. **108**, 141103 (2016).

[7] P.M. Coulon, M. Mexis, M. Teisseire, M. Jublot, P. Vennéguès, M. Leroux, and J. Zuniga-Perez, J. Appl. Phys. **115**, 153504 (2014).

[8] K. Kishino and S. Ishizawa, Nanotechnology **26**, 225602 (2015).

[9] C. Köpler, M. Sabathil, F. Römer, M. Mandl, M. Strassburg, and B. Witzigmann, Phys. Status Solidi **11**, 2304 (2012).

[10] X. Dai, A. Messanvi, H. Zhang, C. Durand, J. Eymery, C. Bougerol, F.H. Julien, and M. Tchernycheva, Nano Lett. **15**, 6958 (2015).

[11] N. Guan, X. Dai, A. Messanvi, H. Zhang, J. Yan, E. Gautier, C. Bougerol, F.H. Julien, C. Durand, J. Eymery, and M. Tchernycheva, ACS Photonics 597 (2016).

[12] H. Zhang, X. Dai, N. Guan, A. Messanvi, V. Neplokh, V. Piazza, M. Vallo, C. Bougerol, F.H. Julien, A. Babichev, N. Cavassilas, M. Bescond, F. Michelini, M. Foldyna, E. Gautier, C. Durand, J. Eymery, and M. Tchernycheva, ACS Appl. Mater. Interfaces **8**, 26198 (2016).

[13] K. Kishino, K. Nagashima, and K. Yamano, Appl. Phys. Express **6**, 12101 (2013).

[14] S. Jahangir, M. Mandl, M. Strassburg, and P. Bhattacharya, Appl. Phys. Lett. **102**, 71101

(2013).

[15] R. Wang, H.P.T. Nguyen, A.T. Connie, J. Lee, I. Shih, and Z. Mi, Opt. Express **22**, A1768 (2014).

[16] K. Kishino, A. Yanagihara, K. Ikeda, and K. Yamano, Electron. Lett. **51**, 852 (2015).

[17] R. Koester, J.-S. Hwang, D. Salomon, X. Chen, C. Bougerol, J.-P. Barnes, D.L.S. Dang, L. Rigutti, A. De Luna Bugallo, G. Jacopin, M. Tchernycheva, C. Durand, and J. Eymery, Nano Lett. **11**, 4839 (2011).

[18] T. Schimpke, M. Mandl, I. Stoll, B. Pohl-Klein, D. Bichler, F. Zwaschka, J. Strube-Knyrim, B. Huckenbeck, B. Max, M. Müller, P. Veit, F. Bertram, J. Christen, J. Hartmann, A. Waag, H.-J. Lugauer, and M. Strassburg, Phys. Status Solidi **213**, 1577 (2016).

[19] Y.-H. Ra, R. Navamathavan, J.-H. Park, and C.-R. Lee, Nano Lett. **13**, 3506 (2013).

[20] R. Koester, J. Hwang, D. Salomon, X. Chen, C. Bougerol, J. Barnes, D. Le, S. Dang, L. Rigutti, A.D.L. Bugallo, G. Jacopin, M. Tchernycheva, C. Durand, and J. Eymery, Nano Lett. **11**, 4839 (2011).

[21] C. Durand, C. Bougerol, J. Carlin, G. Rossbach, F. Godel, J. Eymery, P. Jouneau, A. Mukhtarova, R. Butte, and N. Grandjean, ACS Photonics **1**, 38 (2014).

[22] Z. Bi, A. Gustafsson, F. Lenrick, D. Lindgren, O. Hultin, L.R. Wallenberg, B.J. Ohlsson, B. Monemar, and L. Samuelson, J. Appl. Phys. **123**, 25102 (2018).

[23] M.A. Conroy, H. Li, G. Kusch, C. Zhao, B.S. Ooi, E. Paul, R. Martin, J.D. Holmes, and P. Parbrook, Nanoscale **8**, 11019 (2016).

[24] Y. Ra, R. Navamathavan, S. Kang, and C. Lee, J. Mater. Chem. C **2**, 2692 (2014).

[25] Y.J. Hong, C.-H. Lee, A. Yoon, M. Kim, H.-K. Seong, H.J. Chung, C. Sone, Y.J. Park, and G.-C. Yi, Adv. Mater. **23**, 3284 (2011).

[26] X.J. Chen, G. Perillat-Merceroz, D. Sam-Giao, C. Durand, and J. Eymery, Appl. Phys. Lett. **97**, 151909 (2010).

[27] R. Koester, J.S. Hwang, C. Durand, D.L.S. Dang, and J. Eymery, Nanotechnology **21**, 15602 (2010).

[28] J. Eymery, X. Chen, C. Durand, M. Kolb, and G. Richter, Comptes Rendus Phys. **14**, 221 (2013).

[29] C. Tessarek, M. Heilmann, E. Butzen, A. Haab, H. Hardtdegen, C. Dieker, E. Spiecker, and S. Christiansen, Cryst. Growth Des. **14**, 1486 (2014).

[30] D.C. Watson, R. V. Martinez, Y. Fontana, E. Russo-Averchi, M. Heiss, A. Fontcuberta I Morral, G.M. Whitesides, and M. Lončar, Nano Lett. **14**, 524 (2014).

[31] L. Mancini, W. Lefebvre, J. Houard, I. Blum, F. Vurpillot, J. Eymery, C. Durand, and L. Rigutti, Appl. Phys. Lett. **108**, 42102 (2016).

[32] L. Rigutti, I. Blum, D. Shinde, D. Hernández-Maldonado, W. Lefebvre, J. Houard, F. Vurpillot, A. Vella, M. Tchernycheva, C. Durand, J. Eymery, and B. Deconihout, Nano Lett. **14**, 107 (2014).

[33] Y.-H. Ko, J. Song, B. Leung, J. Han, and Y.-H. Cho, Sci. Rep. **4**, 5514 (2015).

[34] B. Damilano and B. Gil, J. Phys. D. Appl. Phys. **48**, 403001 (2015).

[35] D.A. Browne, E.C. Young, J.R. Lang, C.A. Hurni, and J.S. Speck, J. Vac. Sci. Technol. A Vacuum, Surfaces, Film. **30**, 41513 (2012).

[36] P. Horenburg, E.R. Buß, U. Rossow, H. Bremers, F.A. Ketzer, and A. Hangleiter, Appl. Phys. Lett. **108**, 102105 (2016).

[37] S. Keller, B.P. Keller, D. Kapolnek, A.C. Abare, H. Masui, L.A. Coldren, U.K. Mishra, and S.P. Den Baars, Appl. Phys. Lett. **68**, 3147 (1998).

[38] N. Yoshimoto, T. Matsuoka, T. Sasaki, and A. Katsui, Appl. Phys. Lett. **59**, 2251 (1991).

[39] Y.-L. Lai, C.-P. Liu, Y.-H. Lin, T.-H. Hsueh, R.-M. Lin, D.-Y. Lyu, Z.-X. Peng, and T.-Y. Lin, Nanotechnology **17**, 3734 (2006).

[40] H.Y. Peng, M.D. McCluskey, Y.M. Gupta, M. Kneissl, and N.M. Johnson, Phys. Rev. B

71, 115207 (2005).

[41] G. Jacopin, D.L.A. Bugallo, P. Lavenus, L. Rigutti, F.H. Julien, L.F. Zagonel, M. Kociak, C. Durand, D. Salomon, X.J. Chen, J. Eymey, and M. Tchernycheva, Appl. Phys. Express **5**, 14101 (2012).

[42] Y.-H. Ra, R. Navamathavan, H.-I. Yoo, and C.-R. Lee, Nano Lett. **14**, 1537 (2014).

Figure 1

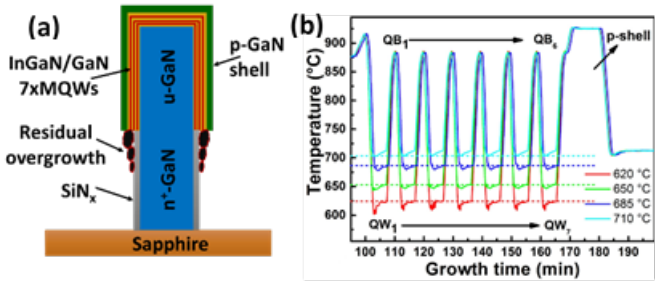
(a)
InGaN/GaN
7xMQWs
p-GaN
shell
u-GaN
Residual
overgrowth
SiNx
n+-GaN
Sapphire
(b)
QB1
QBx
p-shell
Temperature (°C)
900
850
800
750
700
650
600
620 °C
650 °C
685 °C
710 °C
QW1
QWz
100 110 120 130 140 150 160 170 180 190
Growth time (min)

Figure 2

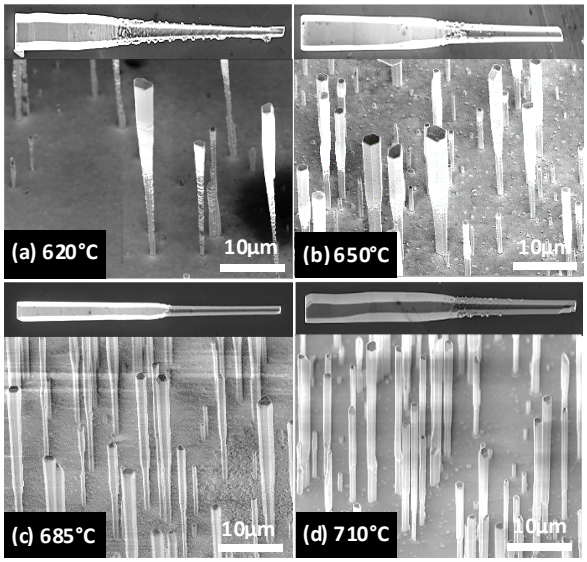

Figure 3

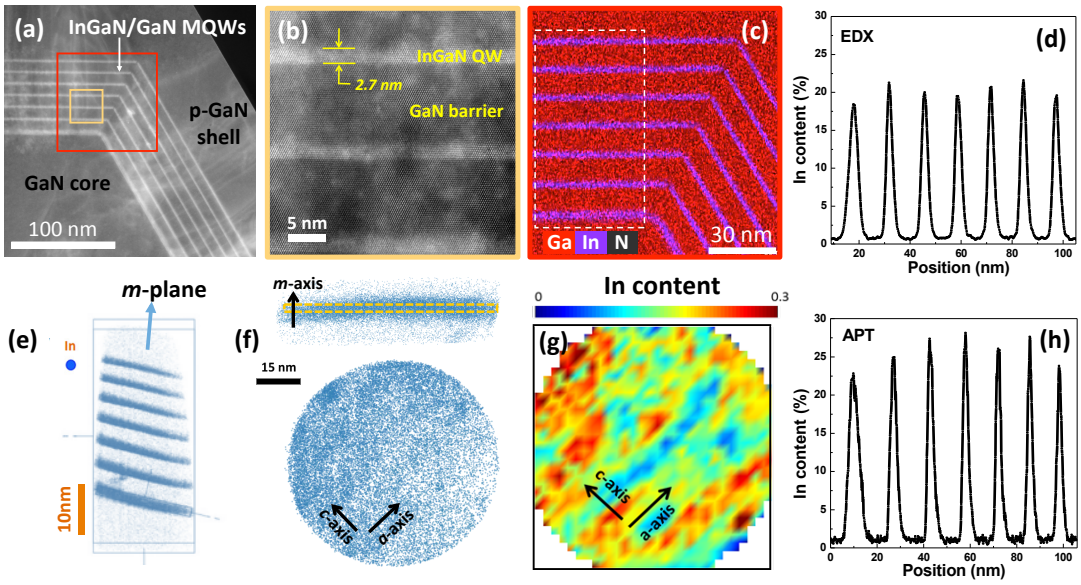
(a)
InGaN/GaN MQWs
p-GaN shell
GaN core
100 nm
(b)
InGaN QW
2.7 nm
GaN barrier
5 nm
(c)
Ga In N
30 nm
EDX
(d)
In content (%)
Position (nm)
m-plane
(e)
In
10nm
m-axis
(f)
15 nm
c-axis
a-axis
In content
0
0.3
(g)
c-axis
a-axis
APT
(h)
In content (%)
Position (nm)

Figure 4

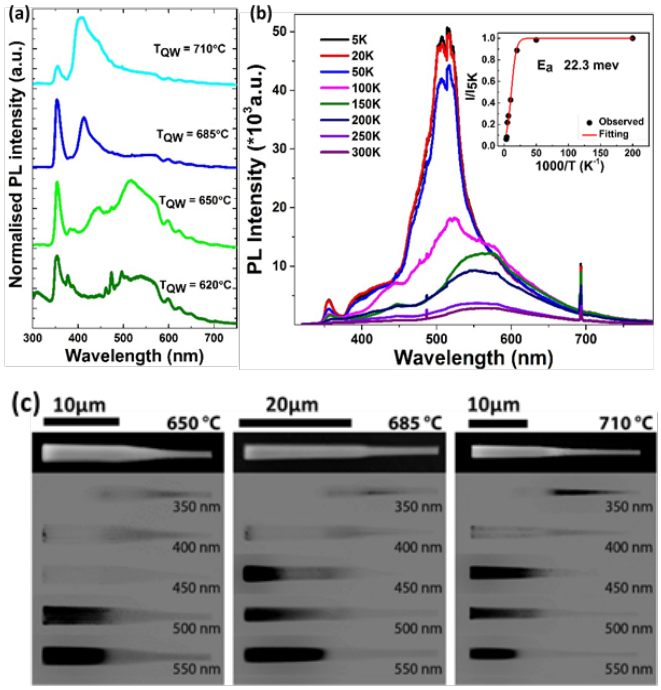
(a)
Normalised PL intensity (a.u.)
T_{QW} = 710°C
T_{QW} = 685°C
T_{QW} = 650°C
T_{QW} = 620°C
300
400
500
600
700
Wavelength (nm)
(b)
PL Intensity (*10^{3}a.u.)
5K
20K
50K
100K
150K
200K
250K
300K
I/I5K
E_a 22.3 mev
Observed
Fitting
1000/T (K^{-1})
400
500
600
700
Wavelength (nm)
(c)
10µm
650 °C
20µm
685 °C
10µm
710 °C
350 nm
400 nm
450 nm
500 nm
550 nm

Figure 5

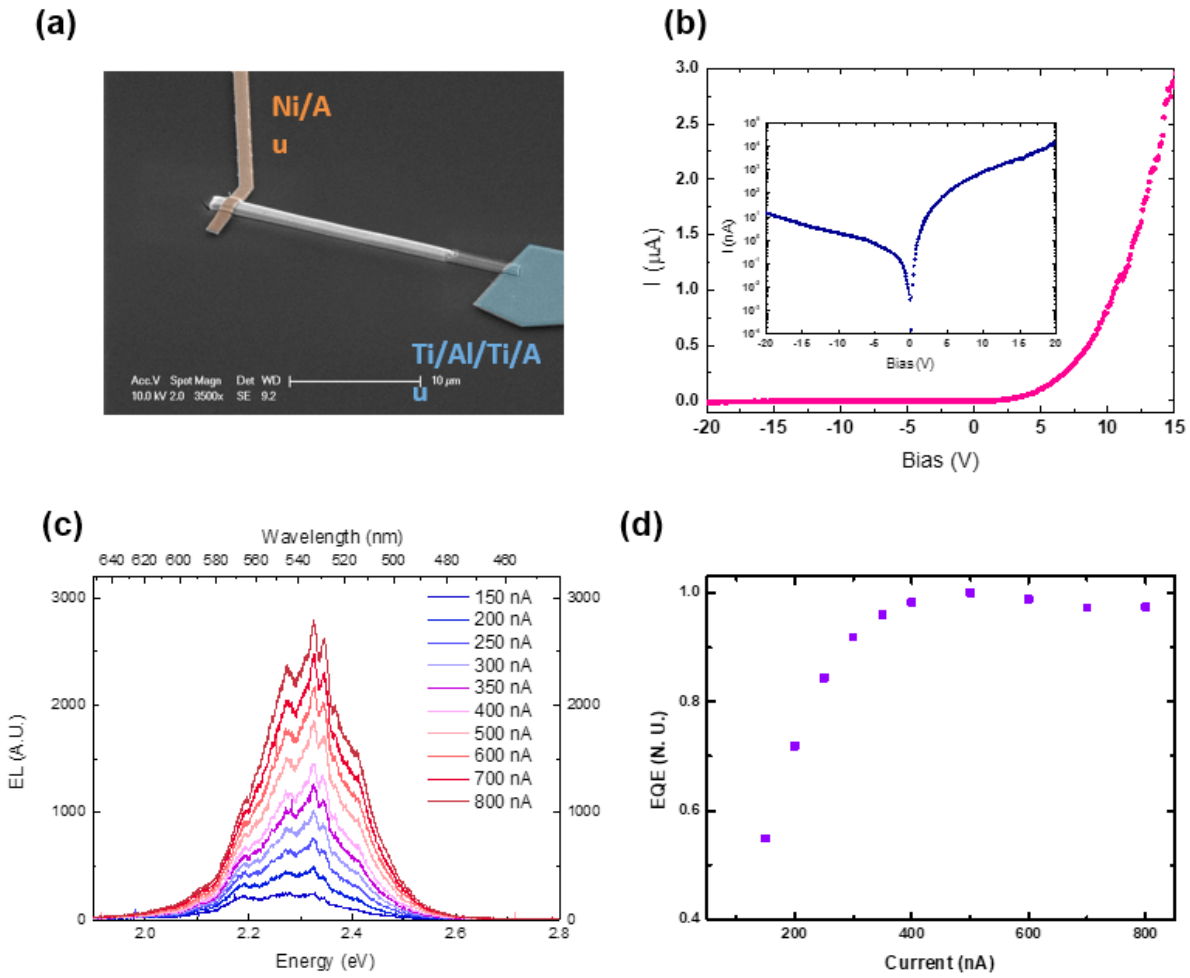
(a)
Ni/A
u
Ti/Al/Ti/A
u
(b)
I (μA)
Bias (V)
I (nA)
Bias (V)
(c)
Wavelength (nm)
EL (A.U.)
Energy (eV)
150 nA
200 nA
250 nA
300 nA
350 nA
400 nA
500 nA
600 nA
700 nA
800 nA
(d)
EQE (N. U.)
Current (nA)